Russian Geology and Geophysics © 2020, V.S. Sobolev IGM, Siberian Branch of the RAS
Vol. 61, No. 7, pp. 738–755, 2020 *DOI:10.15372/RGG2019135* *Geologiya i Geofizika*

Record of the Late Neopleistocene and Holocene Climatic Fluctuations in the Soils of the Upper Angara Region

V.A. Golubtsov[a, ✉], A.A. Cherkashina[a], S.A. Tukhta[a], M.I. Kuz'min[b], A.V. Sizov[c]

[a] *V.B. Sochava Institute of Geography, Siberian Branch of the Russian Academy of Sciences, ul. Ulan-Batorskaya 1, Irkutsk, 664033, Russia*

[b] *A.P. Vinogradov Institute of Geochemistry, Siberian Branch of the Russian Academy of Sciences, ul. Favorskogo 1A, Irkutsk, 664033, Russia*

[c] *Institute of the Earth's Crust, Siberian Branch of the Russian Academy of Sciences, ul. Lermontova 128, Irkutsk, 664033, Russia*

Received 17 January 2019; received in revised form 8 April 2019; accepted 22 May 2019

Abstract—We present results of a study of carbonate coatings formed at the lower surfaces of pebble inclusions in Holocene–Upper Pleistocene deposits of the Irkutsk–Cheremkhovo plain. The coatings resulted from the leaching of carbonates from the overlying deposits during pedogenesis. They are composed of pure and magnesian calcite with minor inclusions of quartz and feldspars. The coatings form morphologically and compositionally different microlayers, which reflect a successive change in the pedogenesis conditions during their formation. The stable-isotope composition is as follows: $\delta^{13}C$ is –6.80 to –2.05‰, and $\delta^{18}O$ is –16.33 to –10.15‰. It reflects the precipitation of carbonates during the degassing of soil solutions in the course of periodic freezing–thawing processes, dynamic increase and decrease in the biological activity of soils, and alternating moistening of soil with meltwater and rain water and its subsequent freezing, which could occur in the region in spring and autumn. A joint analysis of the carbon isotope composition of the organic matter of soils and carbonate coatings shows that the latter formed in the phytocoenosis environment with predominant C3 vegetation. The differences in the morphology and occurrence of the coatings permit them to be divided into three groups. The coatings of the first group formed in the Middle Holocene (3.6–3.3 cal. ka BP), and the coatings of the second and third groups, in the second half of MIS 3 (24.1–23.3 and ~34–35 cal. ka BP, respectively). The paleoecologic conditions reconstructed for the established stages of carbonate coating formation are in satisfactory correlation with the general course of climatic fluctuations in the region and in the Northern Hemisphere as a whole. They reflect the influence of temperature and humidity fluctuations on the dynamics of soil formation processes. Comparison of the age of the coatings with the age of recent and buried soils shows that the pedogenic carbonate coatings in the Upper Angara soils are a relict feature of the previous epochs of pedogenesis (MIS 3) and the first stages of recent soil formation, which began, most likely, in the Middle Holocene. Based on analysis of the rates of coating formation and comparison of the isotope composition of the coatings of different age groups, we assume that the climate in the Karga (MIS 3) megainterstadial was more humid than that in the Middle Holocene, with the temperatures of pedogenesis being the same. Both in the Middle Holocene and in the Karga epoch, the regional soils received little heat and were seasonally frozen for a long time.

Keywords: pedogenic carbonates, paleosoils, stable carbon and oxygen isotopes, radiocarbon age, Late Neopleistocene, Holocene

INTRODUCTION

Exposed and buried soils are an important part of the Quaternary record (Kraus, 1999; Retallack, 2001; Sheldon and Tabor, 2009; Zykina and Zykin, 2012; Tabor and Myers, 2015). They supplement information on sedimentation processes and conditions and contribute to the general picture of development of the environment. They are a significant chronostratigraphic reference, which permits carrying out stratigraphic division of sediments, tracing the chronology of formation of the soil–sediment sequence, and making a correlation of spatially distant strata (Birkeland, 1999; Feng et al., 2011; Zykina and Zykin, 2012; Murphy et al., 2014; Alekseeva et al., 2016; Sauer et al., 2016).

Holocene soils are best preserved in the geologic record, whereas the soils which formed during warm periods of the Pleistocene are preserved much worse. They are often substantially altered by cryogenic processes activated during cold epochs. This favored the disruption of the genetic profile of soils and its characteristic set of morphotypic features (Glushankova, 2010; Zykina and Zykin, 2012), reducing the potential of Pleistocene buried soils as a paleogeographic reference. Such an effect on present-day and Holocene soils is produced by human activity, which often does not permit reconstructing their past formation conditions.

This circumstance makes it necessary to determine stable features which, when changing, mark soil development stages; the evolution–genetic characteristics which can be

✉ Corresponding author.
E-mail address: tea_88@inbox.ru (V.A. Golubtsov)

dated by methods of absolute geochronology are especially valuable as intrasoil records of environmental changes. Carbonates are one of such features; they are a unique group of minerals taking an active part in biological and physicochemical processes through all the geologic epochs (Reeder, 1983). In subaerial deposits carbonates are generally contained in dispersed form. However, during soil formation, carbonate minerals can make up neoformations (secondary carbonate accumulations). They are one of the most important genetic, compositional, and classification components of soils forming in a wide range of natural and climatic conditions (Eswaran et al., 2000). Their formation is closely related to pedogenesis and evolution (Zamanian et al., 2016). The distribution and morphology of pedogenic carbonates in the soil profile reflect the trend and intensity of pedogenesis (Kovda et al., 2003; Khokhlova, 2008). Their isotopic composition can give an insight into paleoclimate, the composition of ancient vegetation (Cerling, 1984; Dworkin et al., 2005; Pustovoytov et al., 2007; Monger et al., 2009; Quade et al., 2013; Oerter and Amundson, 2016), and the dynamics of landforms (Kovda et al., 2006; Quade et al., 2007; Barta et al., 2018). The application of different methods for dating pedogenic carbonates helps to solve geochronology problems (Singhvi et al., 1996; Sharp et al., 2003; Pustovoytov et al., 2007; Khokhlova et al., 2013; Oerter et al., 2016).

Stratified coatings (pendants) are especially promising; their formation resembles the formation of speleothems (Brock and Buck, 2005), which have been viewed in recent years as one of the most promising sources of continental paleoclimate evidence (Fairchild and Baker, 2012). According to (Brewer, 1964), coatings (from Latin *cutis* "skin, rind, surface") are defined as modifications of the soil texture, structure, composition, and profile near interfaces as a result of *in situ* concentration or transformations of the finest and most active soil (plasma) substances. Thus, the term "coating" characterizes primarily the confinement of this class of soil neoformations to an interface (surface of mineral grains, pores, and aggregates). This group of pedogenic (generally speaking, exogenous) neoformations is formed by a vertical (radial) flow of gravity moisture transporting dissolved and suspended matter of different compositions within soil (weathering crust or eluvium). Coatings, which are formed by consecutive deposition from illuviated solutions and suspensions, are the best example of illuviation (Bronnikova, 2008). A large, genetically important group is made up of illuviation coatings, the main component of which is carbonate.

Actually, layered carbonate coatings are microsedimentation systems within the soil profile formed by within-profile migration of substances in true solutions, colloidal solutions, and suspensions and by their deposition on geochemical and mechanical barriers within soil (Bronnikova et al., 2017). Differences in the compositions of solutions and suspensions in migration and deposition conditions lead to the formation of structurally and compositionally different coatings. So, complex coatings are a specific source of evidence containing a layer-by-layer record of the trend, intensity, and succession of within-profile migration and accumulation of material as well as the environment determining these processes (Courty et al., 1994; Pustovoytov, 2002; Oerter et al., 2016; Zamanian et al., 2016; Bronnikova et al., 2017; Golubtsov, 2017).

The studies conducted by the authors in recent years (Golubtsov et al., 2014; Golubtsov, 2017) have shown the widespread occurrence of these neoformations in soils of the Upper Angara region. However, their potential for paleopedological and paleogeographical reconstructions has not been used as yet. The present paper is aimed at reconstruction of the dynamics of soil formation conditions and its relationship with Late Neopleistocene and Holocene climate fluctuations from studies of the occurrence, morphology, material and isotopic compositions, and ^{14}C age of pedogenic carbonate coatings in soils of the Upper Angara region.

SUBJECTS AND METHODS

The studies were conducted in the southern Irkutsk Region, within the Irkutsk–Cheremkhovo Plain, mainly in the lower reaches of the Belaya River (tributary of the Angara River) (Fig. 1). The territory is characterized by extra-continental climate. The mean annual temperature is 1 °C; the average July temperature, +18.3 °C; the average January temperature, –17.8 °C. The annual precipitation is 480 mm, ~80% of which falls out in late July and August. From late May to middle July, dry and warm conditions predominate in the area (Irkutsk Climate, http://www.pogodaiklimat.ru/climate/30710.htm).

Most of the lands in the study territory are arable, and undisturbed areas are occupied by meadow steppe forb–grass vegetation and sparse mixed woodlands. The predominating soils are Luvic Chernozems formed on loesslike loams (The Irkutsk–Cheremkhovo…, 1969).

Geologically, the territory in the lower reaches of the Belaya River consists of Cambrian, Jurassic, Cretaceous–Paleogene, Oligocene–Miocene, Pliocene, Pleistocene, and Holocene rocks (Antropov, 1962). The lower Cambrian strata are tabular gray siliceous dolomites and limestones. The Jurassic rocks are present as Lower Jurassic conglomerates, sandstones, and siltstones and Middle Jurassic coal-bearing siltstones, mudstones, and sandstones (Antropov, 1962). The Oligocene–Miocene strata are composed of poorly cemented sandstones, pebble gravel with kaolin fill, and weathering crust fragments. The Pliocene–Miocene deposits fill fragments of the gully network incised in the Jurassic basement in multiple-elevation areas (445–420 m) (Florensov, 1971). The Pleistocene loose sediments overlie the above-mentioned pre-Quaternary rocks at watersheds as a thin cover, but their thickness increases considerably within the valley, where terraces of different ages are distinguished (Logachev et al., 1964).

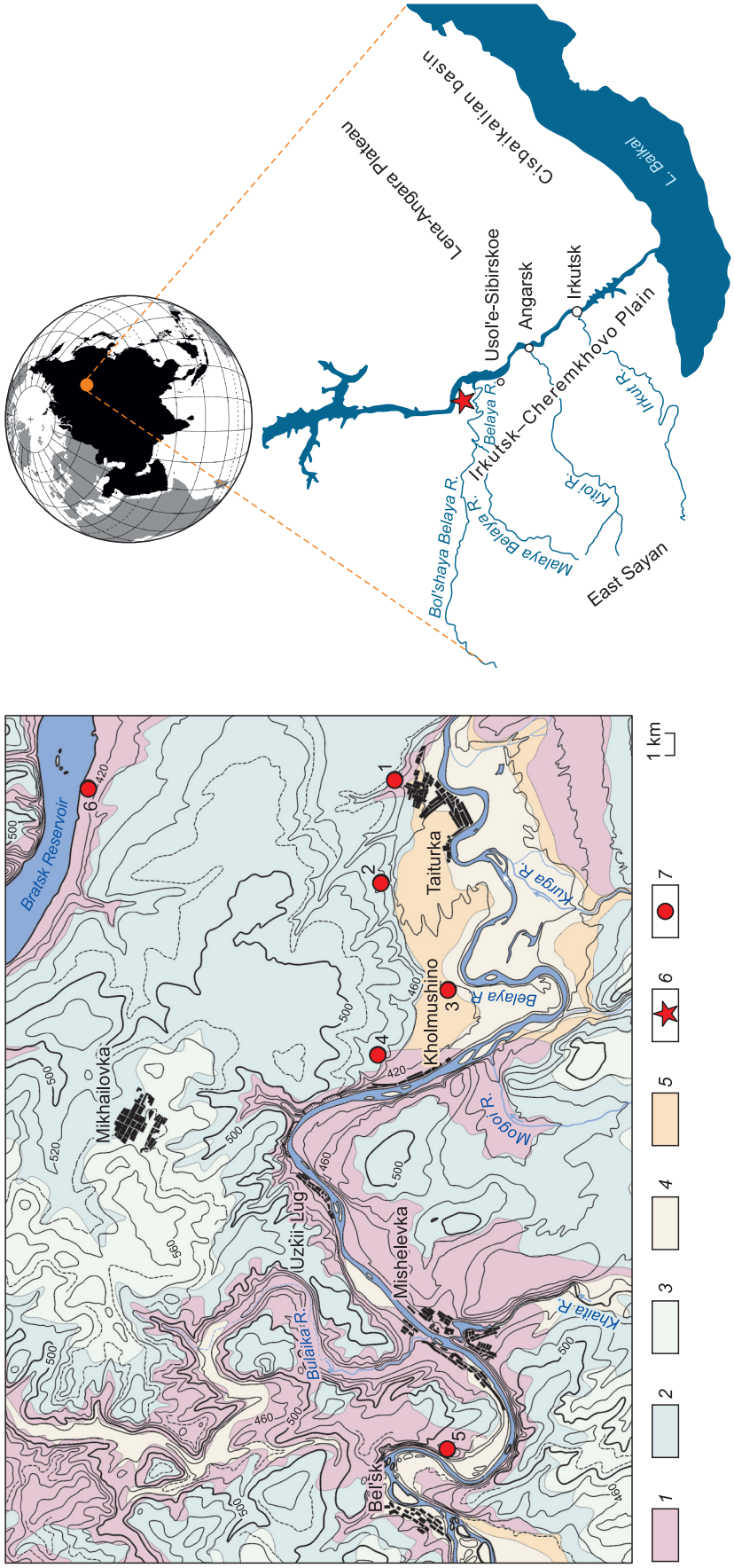

Fig. 1. Study area and positions of sections: *1*, Taiturka I; *2*, Taiturka II; *3*, Berezovyi; *4*, Osinovyi; *5*, Lower Bulai II; *6*, Buret'. *1*, lower Cambrian dolomites, limestones, and marls; *2*, Lower Jurassic conglomerates, breccias, sandstones, and clays; *3*, Middle Jurassic arkosic sandstones, quartz siltstones, mudstones, and coal beds; *4*, Quaternary alluvial deposits, loams, sandy loams, clays, and silts with pebbles, pebble deposits; *5*, Quaternary alluvial and alluvial–talus deposits; *6*, study area; *7*, study sections.

In the lower reaches of the Belaya River, the following areas are observed: (1) small neotectonic highs with an intermittent regime of accumulation and denudation, (2) areas of small neotectonic lows and stability with predominant accumulation till the Late Pleistocene, and (3) the largest neotectonic lows with predominant accumulation in the Pleistocene and Holocene. The largest lows form local depressions separated by highs or small lows. The biggest one, the Bel'sk depression, adjoins the study area in the west and is separated by an uplift coinciding with the axis of a Cambrian coeval anticline. From west to east, the following depressions are distinguished, respectively: Khaita–Bulai, Kholmushino–Taiturka, Mal'ta, and Ust'-Belaya (Vorob'eva and Medvedev, 1985).

The group of low terraces and the floodplain of the Belaya River formed only within the depressions. In the rest of the areas, the riverbed has an erosion–tectonic character with steep scarps of the dolomite basement. The riverbed structure coincides with regional rift directions: long northwestern and short northeastern areas. Meandering is also pronounced only in depression areas (Vorob'eva and Medvedev, 1985).

The present study is based on data from six sections of loose deposits. The Taiturka I section (52°52′ N; 103°28′ E; elevation 434 m a.s.l.) exposes the structure of the talus cone overlying the alluvial deposits of the third terrace of the Belaya River. The Taiturka II section (52°52′ N; 103°25′ E; elevation 436 m a.s.l.) strips the oxbow depression replacing the back suture of the third terrace, which is now buried under a thin talus cone. In the Berezovyi section (52°51′ N; 103°21′ E; elevation 417 m a.s.l.), we studied the structure of carbonate loesslike loams overlying the strongly carbonate-enriched gravel–pebble bed alluvium of the second terrace of the Belaya River. In the Osinovyi section (52°53′ N; 103°19′ E; elevation 460 m a.s.l.), the third terrace of the Belaya River is exposed. Now the section area looks like a draw terrace. A thin (about 2 m) cover of loesslike deposits is here underlain by variegated alluvium with a dolomite basement. The Lower Bulai II section (52°51′ N; 103°06′ E; elevation 496 m a.s.l.) exposes loesslike loams overlying a buried soil profile which formed on ferruginous and carbonate-enriched pebble gravel with sand and loam fill. The Buret' section (52°58′ N; 103°28′ E; elevation 403 m a.s.l.) is localized on the left bank of the Angara River and strips its first terrace, which consists of thin sandy loam strata underlain by sandy pebble gravel with a dolomite basement.

Field studies focused on stratigraphic and morphogenetic analysis of deposits and buried soils as well as analysis of distribution of carbonate coatings in the sections. In the laboratory, samples of host soils and deposits were made air-dry, crushed, and put through a sieve (1 mm). The content of carbonate CO_2 was found acidimetrically, and that of total organic carbon was found by dry combustion on a Vario Isotope analyzer (Elementar, Germany). Grain size composition was determined with the use of the average sample in stagnant water by the pipette method (after N.A. Kachinskii). The age of buried soils was determined by radiocarbon dating with scintillation counting of activity of ^{14}C based on humic acid carbon at St. Petersburg State University.

Carbonate coatings were collected together with pebble inclusions on which they had been formed. Under laboratory conditions each pebble unit was cut with a petrographic saw into slides 5–7 mm thick perpendicularly to the greatest length of the coating. The obtained sections of carbonate neoformations were later used in studies.

To measure the ratios of stable carbon and oxygen isotopes, coating material was drilled out of the outer and inner layers detected microscopically in the sections. The measurements were taken on a Thermo Finnigan MAT 253 mass spectrometer with a GasBench II system at the Center for Shared Facilities for Multielement and Isotope Studies (Sobolev Institute of Geology and Mineralogy, Novosibirsk) and on a Thermo Finnigan MAT 252 mass spectrometer at the University of Tübingen (Germany).

The composition of stable carbon isotopes in soil and paleosoil organic matter was determined after the removal of roots, detrital inclusions, and carbonates at the Center for Shared Access "Laboratory of Radiocarbon Dating and Electron Microscopy" (Institute of Geography, Russian Academy of Sciences, Moscow) on an Elementar Isoprime precisION IRMS (United Kingdom). The results of all the isotope measurements are presented in per mil (‰) with respect to the VPDB standard, with an accuracy of 0.1‰.

The inner and outer layers of the coatings were separated from one another under a microscope and crushed to powder in an agate mortar. The mineral composition of unoriented samples was determined on a Bruker AXS D8 Advance diffractometer (Germany). The elemental composition of the coating layers was determined on a Bruker AXS S4 Pioneer XRF spectrometer.

Mesomorphological studies were conducted using a Micromed MC-2-ZOOM microscope. Submicroscopic studies and point layer-by-layer probing of neoformations were carried out on an EDS at the Center for Shared Access "Laboratory of Radiocarbon Dating and Electron Microscopy" (Institute of Geography, Russian Academy of Sciences, Moscow) using a JEOL JSM-6610LV SEM (Japan) with Oxford INCA Energy and Oxford INCA Wave analyzers. Fresh fractured surfaces were studied after Au sputtering.

Coating layers marking a change of soil formation stages were used for ^{14}C AMS dating with a MICADAS in the laboratory of Klaus-Tschira-Archäometrie-Zentrum (Mannheim, Germany). Hereinafter, calibrated ^{14}C ages are presented; the calibration is carried out against the INTCAL13 scale.

RESULTS

Structure, physicochemical properties, and age of the studied soils and deposits. The studied sections expose thin (0.7–5 m) strata of cover loesslike loams and sandy loams underlain by different-aged alluvium (Fig. 2). In the Berezovyi, Lower Bulai II, and Buret' sections, it consists of

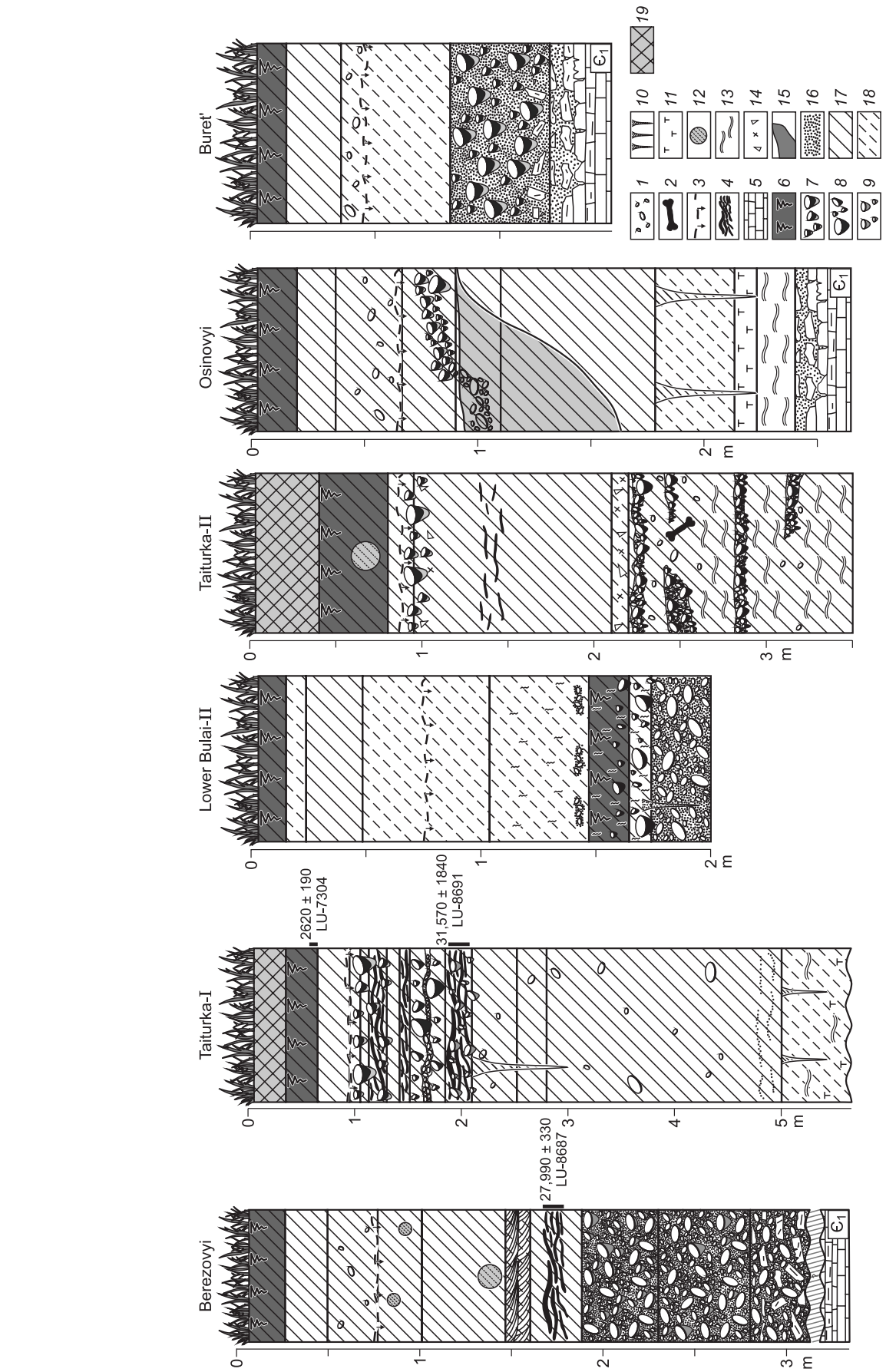

Fig. 2. Structure and radiocarbon age of deposits from the studied sections. *1*, pebble inclusions; *2*, fossil bones; *3*, upper boundary of the carbonate profile; *4*, pedosediments; *5*, bedrocks; *6*, humus horizons of surface soils; *7–9*, carbonate coatings of groups I, II, and III, respectively; *10*, cryogenic wedges; *11*, peat interbeds; *12*, mole burrows; *13*, clay interbeds; *14*, gruss and rubble inclusions; *15*, buried erosional form; *16*, sands; *17*, loams; *18*, sandy loams; *19*, anthropogenic deposits.

sandy pebble gravel overlying Paleozoic rocks with an abrupt contact. In the Taiturka I and Osinovyi sections, cover loesslike deposits are underlain by crossbedded loose white sandstones intercalated with clays and carbonized fine plant detritus (most probably, of Jurassic age), which overlie Lower Cambrian deposits. The lower part of the Taiturka II section exposes middle- to coarse-grained loams intercalated with sandy gravel–pebble beds and clays.

The cover loesslike deposits in almost all the studied sections exhibit traces of past soil formation as humic pedosediments at a depth of 1.5–2.0 m, dated at the Karga age (MIS 3). For example, the described pedosediments are dated at 27,990 ± 330 cal. yr BP (LU-8687) in the Berezovyi section and 31,570 ± 1840 cal. yr BP (LU-8691) in the Taiturka I section (Fig. 2). The age of the pedosediments from the Taiturka II section is determined using Late Pleistocene faunal fossils below in the section. The bones found are mostly fragmented, with no visible traces of processing by humans. Identifiable, best preserved remains belong to the wild horse (*Equus ferus*) (incisor and proximal phalanx), bison (*Bison priscus*) (astragalus, proximal phalanx, and tibia of a young individual with a nonadherent proximal epiphysis), reindeer (*Rangifer tarandus*) (skull fragment), and mammoth (*Mammuthus primigenius*) (tooth, teeth fragments, and fragment of a long bone) (Fig. 3). All the fauna is typical of the Late Pleistocene in Cisbaikalia (Ermolova, 1978; Klement'ev, 2013). The integrity of the remains, along with the faunal assemblage, suggests their Late Karga–Early Sartan age (MIS 2–MIS 3 boundary). As the morphology and occurrence of the described pedosediments are similar to those of the pedosediments from the sections in immediate proximity, the fossil soils of the Taiturka II section are, most probably, of the Late Karga age.

The taxonomic assignment of the studied Karga (MIS 3) soils is hard, because the system of horizons making up the soil profile was destroyed by past active cryogenic process-

Fig. 3. Fossil bones from the Karga (MIS 3) deposits. *a*, Tibia of a young *Bison priscus* individual; *b*, tooth of *Mammuthus primigenius*; *c*, proximal phalanx of *Bison priscus*; *d*, proximal phalanx of *Equus ferus*; *e*, astragalus of *Bison priscus*.

es. The surface soils forming in the upper parts of the sections are clay–illuvial chernozems (Taiturka I, Taiturka II, and Berezovyi sections) and gray soils (Lower Bulai II, Osinovyi, and Buret' sections). In the Taiturka I section, a ^{14}C age of 2620 ± 190 cal. yr BP (LU-7304) was obtained for the bottom of the humus horizon of chernozem.

The studied sections are characterized by similar distribution of total organic carbon (C_{org}). Its content decreases drastically with increasing depth, with subsequent small peaks corresponding to the humus horizons of fossil soils (Fig. 4). The distribution of carbonates has the following characteristics. The carbonate-rich (BCA) horizons of surface soils are distinct and have a sharp upper boundary, which coincides with the level of effervescence from HCl and is localized at a depth of 70–100 cm from the day surface (Fig. 4). The average thickness of the carbonate-rich horizon is 50 cm. The primary illuvial peak of carbonate content, related to their leaching during present-day pedogenesis, is usually the maximum. As we move down the profile, carbonate content increases many times, generally in the middle horizons of different-aged buried soils. This served as a basis for distinguishing secondary illuvial peaks of carbonate content related to carbonate redistribution during the Late Pleistocene soil formation stages (Fig. 4). The highest calcium carbonate contents are observed in the upper horizons of soils forming in conditions of near-surface occurrence of carbonate-bearing parent rocks (dolomites and limestones). This takes place in the Buret' section.

In general, the carbonate profile of the studied soils formed long ago and is quite unchanged, as evidenced by the undeveloped migration zone, predominant stable forms of carbonate accumulations, absent migration forms, and advanced (for this carbonate content) stage of evolution of the carbonate profile. In most of the studied soils, the development of the carbonate profile is estimated (Chadwick and Graham, 2000) as stage II–II+ (continuous carbonate coatings on pebbles; host fine soil is light-colored because of carbonates and contains 10–25% $CaCO_3$). Dating of carbon-

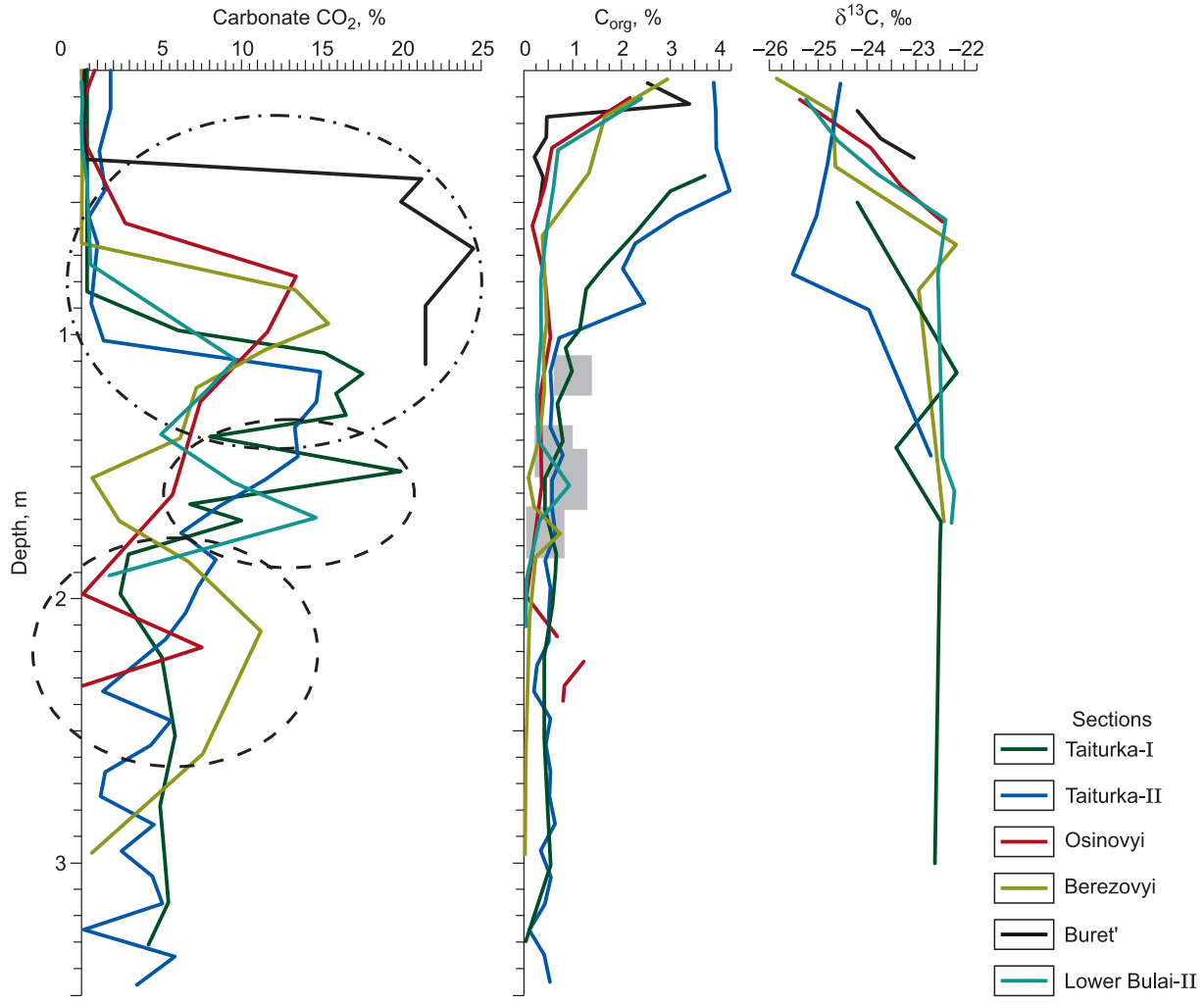

Fig. 4. Carbonate and organic carbon distribution and isotopic composition of organic matter from soils of the studied sections. Gray rectangles show the position of the humus horizons of buried soils.

ate accumulations confirms the great age of the carbonate profile of soils ("Discussion").

Distribution, morphology, and mineral and elemental compositions of carbonate coatings. Pendants are detected both within the BCA horizons of surface soils and at older levels of pedogenesis. They are always localized on the lower surfaces of pebble inclusions. In combination with the carbonate distribution pattern in the profile, this suggests that the coatings formed in the course of carbonate leaching from the overlying deposits during pedogenesis.

Differences in the morphology and occurrence of neoformations permit their subdivision into three groups. In the central and lower parts of the Berezovyi and Taiturka I sections (MIS 3), the coatings of group III are observed. Above in the section, the neoformations of group II are localized (Taiturka I, Taiturka II, and Lower Bulai II sections). The carbonate coatings of group I are detected within the carbonate-rich horizon of the surface soils in the Osinovyi, Taiturka I, Taiturka II, and Buret' sections (Fig. 2).

Group I is divided into several layers of different morphologies and compositions, reflecting the succession of pedogenetic conditions during the coating formation. The phase composition of this group is dominated by Mg-calcite with the main interplanar spacing of 3.01 Å, containing considerable quantities of quartz and feldspars. This group has a high content of SiO_2 (42%), CaO (17%), and iron and aluminum sesquioxides (15%). A compact inner ocherous layer up to 0.5 mm thick is detected in the best developed pendants of this group at the contact with the pebble beds. With a sharp boundary, it passes into the unstratified compact dark brown (5 YR 5/4) middle layer up to 3 mm thick. In turn, it passes, with a sharp pockety boundary, into the unstratified porous brownish gray (2.5 Y 6/2) outer layer (Fig. 5*a*). The inner and middle layers are enriched in organic matter and, to some extent, in iron, suggesting active illuviation of these components into the BCA horizon during the formation of these layers. Carbonate in the coating outer layers does not contain these admixtures. At the submicroscopic level, the structure of the layers is similar. The brown inner layers are composed of close-packed radially fibrous micrite–microsparitic calcite crystals forming spherulites. These spherulites reach 100 μm in diameter, with quartz and feldspar grains as cores (Fig. 6*a*). Local zones of dissolution and recrystallization are observed, with a cellular texture and numerous platy rhomboid calcite crystals degraded to fibers of up to 1 μm. The spherulites in the outer layers are considerably smaller (up to 10–15 μm) (Fig. 6*b*), with much less pronounced crystal etching and dissolution. Particles of the host sediments are often accreted during the coating formation, as evidenced by inclusions of silicate grains dispersed in the neoformations to different extents.

The thick multilayered carbonate coatings of group II (Fig. 5*b*,*c*) are marked by loose thin (up to 3 mm) white (10 YR 9.5/2) outer layers. The coating groundmass is composed of microstratified pigmented middle layers up to 1 cm in thickness. The microlayers are inhomogeneously pigmented: from 7.5 YR 4/4 brown and 7.5 YR 4/6 strong brown to 7.5 YR 6/4 light brown. In many coatings, the microlayers contain etched textures looking as sharp pockety boundaries between the intercalations. The grayish brown (7.5 YR 4/3 brown) inner layer is distinguished at the contact with pebble entities. It sometimes forms in the place of a void, which suggests partial dissolution of the neoformation (Fig. 5*b*, top). The coatings consist of pure calcite with the main interplanar spacing of 3.02 Å, with no admixtures or inclusions of other minerals. Their composition is dominated by CaO (49.41%), with minor quantities of SiO_2 (1.58%), Al_2O_3 (0.5%), and MgO (1.65%).

In the inner layers, etched zones are observed; therefore, rhomboid calcite crystals recrystallize here into fiberlike entities, and the general crystal orientation becomes disordered (Fig. 6*c*). The inner layers are composed of close-packed spherulites, but radially fibrous aggregates are smoothed away from the surface by cryptocrystalline colloform calcite (Fig. 6*d*). The outer layers of the coatings consist of loosely packed, randomly oriented platy or tabular micritic crystals.

The coatings of groups II and III are structurally similar under a binocular microscope (Fig. 5*b*,*e*). The neoformations are very thick, mainly because of the pigmented inner layer, which is divided into numerous microlayers. The white outer layer is of minor thickness. However, submicromorphological studies reveal some differences. The random orientation and loose packing of micritic calcite crystals are also observed in the outer layers of the coatings of group III (Fig. 6*c*). At the same time, the microstratified inner layers of the coatings of this group consist of very closely packed large (up to 100 μm or more) compound carbonate spherulites (Fig. 6*e*). Each of these spherulites is made up of numerous thin (up to 10 μm) layers of radially oriented microsparitic calcite crystals (Fig. 6*f*). The coatings are composed of pure calcite with the main interplanar spacing of 3.02 Å containing quartz admixtures.

Radiocarbon age of carbonate coatings. The radiocarbon age of pedogenic carbonates is influenced by fluctuations of the atmospheric content of ^{14}C. The content of ^{14}C at the moment of carbonate crystallization in soil might be lower than atmospheric content, which leads to the overestimation of radiocarbon age. Till the late 1980s, this was explained by "the limestone dilution effect" (Williams and Polach, 1971; Chen and Polach, 1986). Later, it was found that this mechanism plays a limited role for pedogenic carbonates, because secondary carbonates in soils form in isotope equilibrium with soil-respired CO_2 (Cerling, 1984). Hence, the $^{14}C/^{12}C$ ratio in pedogenic carbonates at the moment of their crystallization corresponds to the atmospheric value (Amundson et al., 1994; Wang et al., 1996). Nevertheless, the use of calibrated dates is preferable to prevent distortions of carbonate age.

The age of pedogenic carbonates might be overestimated because of the supply of older carbon by inclusion of particles of lithogenic carbonates in neoformations (Deutz et al., 2002). However, no such inclusions were detected in our

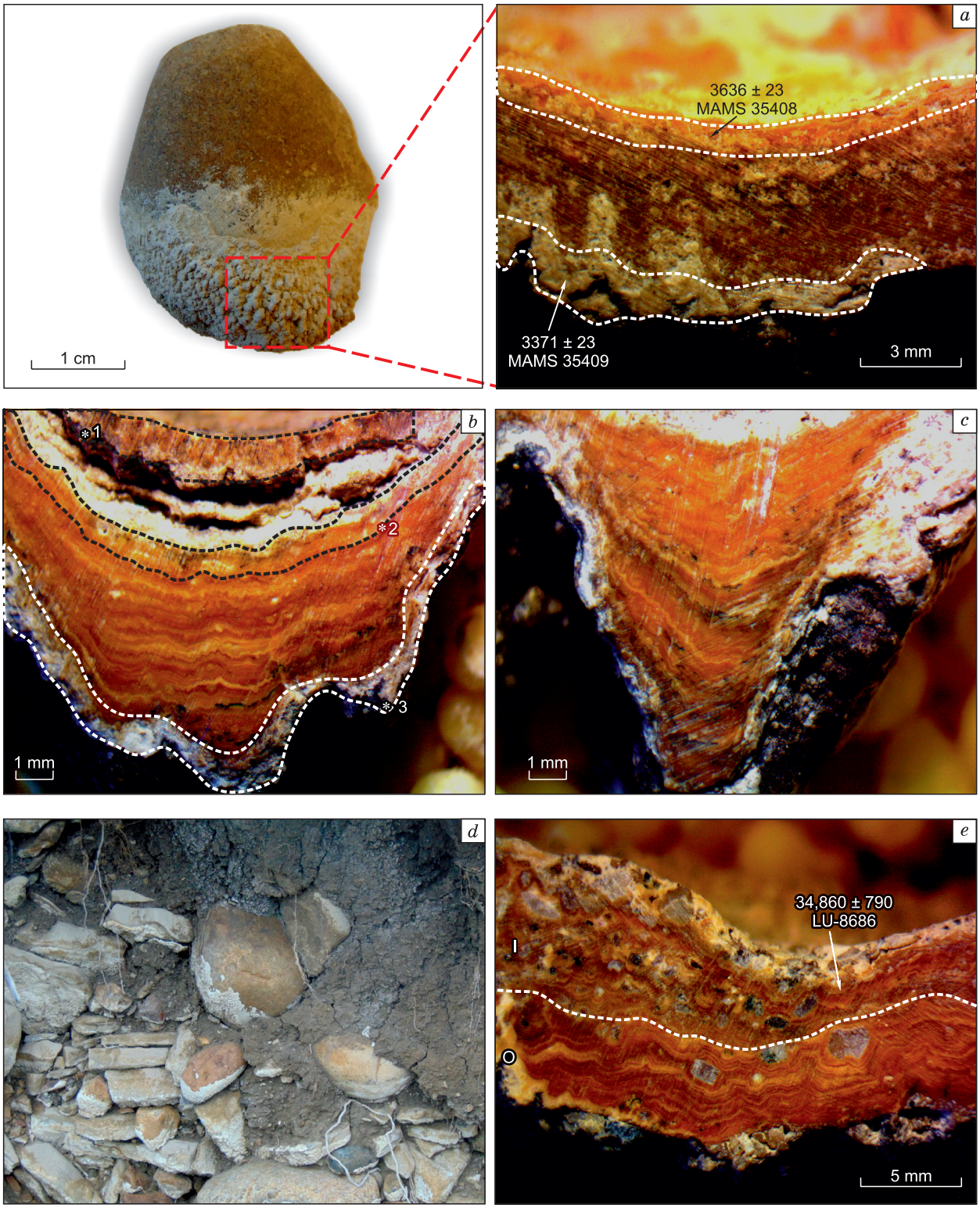

Fig. 5. Structure and radiocarbon age of the main groups of carbonate coatings. *a*, Macro- and mesomorphology of the carbonate coatings of group I; *b*, mesomorphology of the carbonate coatings of group II. ^{14}C-AMS dates (cal. yr BP): *1, 23,189±70 (MAMS-35410), *2, 24,108±70 (MAMS-35411), *3, 23,292±70 (MAMS-35412); *c*, structure of microstalactites forming on the surface of the coatings of group II; *d*, position of carbonate coatings on the lower surfaces of pebble inclusions; *e*, structure of the carbonate coatings of group III. I, inner layers; O, outer layers.

studies of the morphology and mineral composition of carbonate accumulations.

Also, the age of secondary carbonate accumulations might be overestimated because of the influence on pedogenic carbonates exercised by groundwater depleted in ^{14}C as a result of interaction with older carbonate rocks (Deutz et al., 2002). Apparently, this is not a factor in our case: The studied sections exhibit no features of hydromorphism.

Finally, carbonate formation in soils is a cumulative process which might be interrupted by intervals of partial dissolution. The dissolution and subsequent recrystallization of carbonates at small depths (<40 cm) in soils might affect the content of ^{14}C in pedogenic carbonates (Pendall et al., 1994) via inclusion of fresh atmospheric CO_2 in the newly formed crystals. Thus, the age of carbon in carbonate neoformations of complex structure, including coatings, can take an average value for all the crystals in the fraction chosen for analysis. Therefore, we took geochronological measurements in the smallest accessible samples to minimize artificial homogenization of different-aged crystals. Besides that, successive accumulation of coating material, which causes the overlap of older layers by new carbonate material, reduces the contact of the older layers with the external environment. In turn, this reduces the possibility of dissolution and redeposition of the material of pendants, which might decrease possible fluctuations in their ^{14}C age.

The main factor causing the underestimation of the age of pedogenic carbonates is probably the effect of precipitation which carries "young" dissolved CO_2 and weak organic acids through the soil profile, thus favoring in situ dissolution and recrystallization of the carbonate material of neoformations (Khokhlova et al., 2013). However, the carbonate profile of the studied soils, with numerous intraprofile $CaCO_3$ maxima related to multiple carbonate redistribution during diachronous pedogenesis stages, suggests that these processes had no strong impact on the neoformations under study. Each $CaCO_3$ peak above or below is separated by an interval of adrupt decrease in $CaCO_3$ content. Since the soil carbonate profile is a visible reflection of hydrothermal regime, the infiltration of moisture and dissolved CO_2 at each soil formation stage thereafter was limited to the carbonate-rich horizon, so that young carbon within CO_2 did not penetrate deeper layers.

Also, the validity of the obtained dates is confirmed by the fact that age in all the groups of neoformations becomes younger from inner to outer layers, which is logical if we take into account that the carbonate material of pendants accumulates successively. However, as it was said above, voids partly filled with carbonate are sometimes observed in the oldest neoformations of groups II and III at the contact with pebble. The dating of this material showed an inversion of radiocarbon age (Fig. 5*b*), which had been described in (Brock and Buck, 2005). This suggests that carbonate coatings are open to exogenous processes and the dated carbonate needs a thorough morphological analysis.

The ^{14}C-AMS dates obtained for the coating layers (Fig. 5; Table 1) show that the age of the neoformations corresponds to that of the host sediments. Comparison between the ages of the carbonate coatings of group I (3.6–3.3 cal. ka BP) and humic acids from the bottom of the humus horizon (2.6 cal. ka BP) indicates that the coatings formed during early present-day pedogenesis. This conclusion is based on the assumption that a mature chernozem profile forms for about three thousand years (Aleksandrovskii, 2008) and the possibility that organic matter becomes younger during carbon exchange in the biological cycle. The underestimation of the humus age can reach 20% in forest-steppe conditions (Alexandrovskiy and Chichagova, 1998), but this value might be smaller because of the dry conditions in the study area and subzero average annual temperatures. It is estimated that the coatings of group I formed for 300 years. The rate of their formation (the average thickness of the coatings of this group being 6 mm) is 2 mm/100 years. They are relict features reflecting the early formation conditions of present-day chernozems in the study area. Such features are crucial for study of the evolution of well-developed polygenetic soils, since information on early pedogenesis wears out with time (Targul'yan, 2008). Also, they are important in terms of human impact on surface soils, which often does not permit reconstructing their past formation conditions.

The coatings of group II, localized in the BCA horizon of the Late Karga soils, yield the age of 24.1–23.3 cal. ka BP. It is estimated that they formed for 800 years, the carbonate

Table 1. Radiocarbon and calendar ages of carbonate coatings

Laboratory number	Section, group, and coating layer	Dated objects	^{14}C age, yr BP	Interval of calendar age, BP, (probability, %)
MAMS-35408	Osinovyi, group I, inner layer	Carbonate carbon	4861 ± 23	3695–3636 (95.4)
MAMS-35409	Osinovyi, group I, outer layer	Carbonate carbon	4678 ± 23	3620–3612 (1.4) 3521–3483 (22.8) 3476–3370 (71.1)
MAMS-35410	Taiturka II, group II, inner layer	Carbonate carbon	21,000 ± 70	23,618–23,190 (95.4)
MAMS-35411	Taiturka II, group II, middle layer	Carbonate carbon	22,070 ± 70	24,579–24,109 (95.4)
MAMS-35412	Taiturka II, group II, outer layer	Carbonate carbon	21,110 ± 70	23,716–23,291 (95.4)
LU-8686	Berezovyi, group III, inner layers	Carbonate carbon	30,690 ± 780	34,860 ± 790

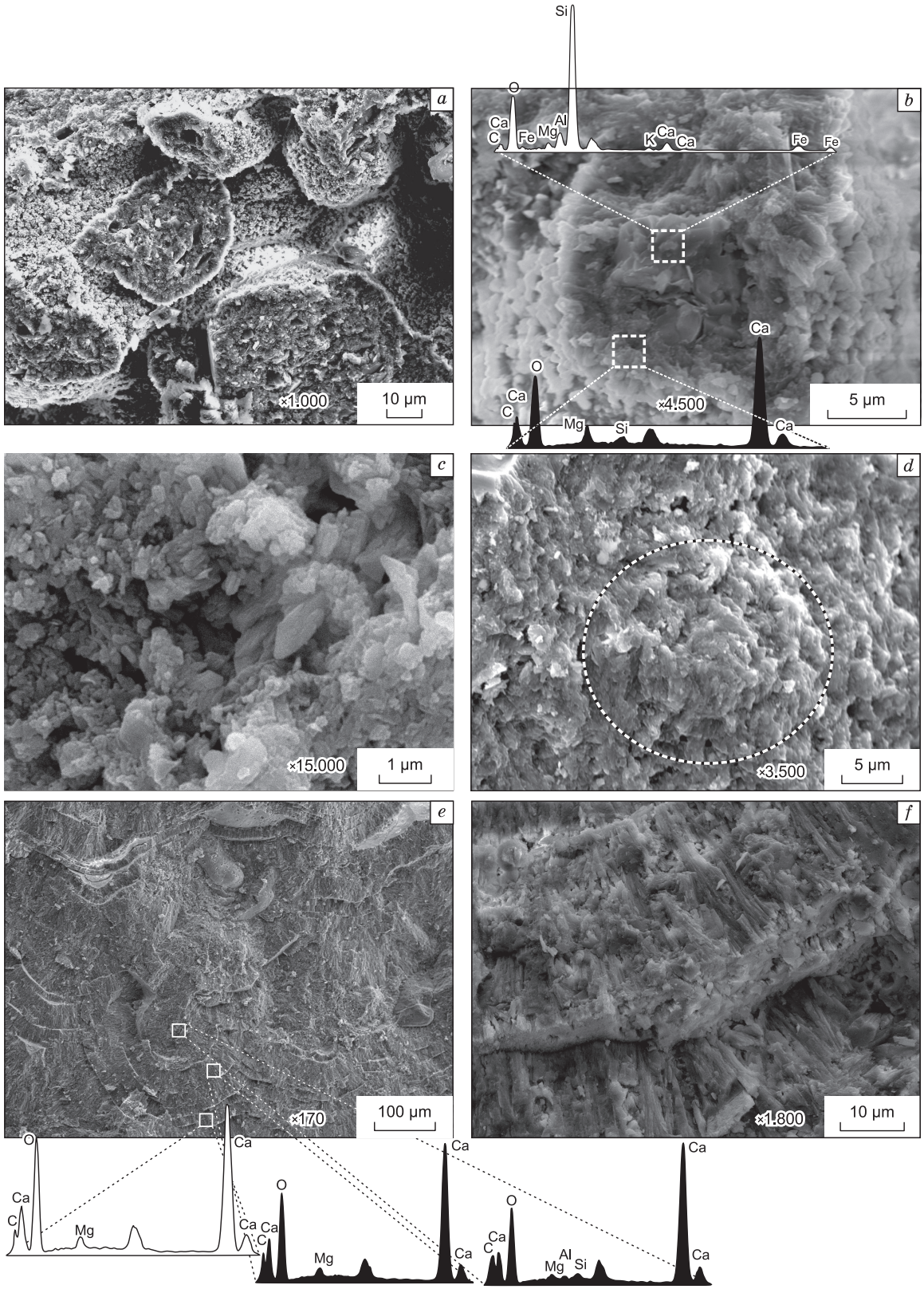

Fig. 6. Submicromorphology and composition of the studied carbonate coatings. *a*, Organization of carbonate material of the inner layers in the coatings of group I; *b*, carbonate spherulites in the outer layers of the coatings of group I; *c*, random orientation of calcite crystals in the etched zones of the outer layers of the neoformations of groups I and II; *d*, spherulites smoothed down by colloform cryptocrystalline calcite in the inner layers of the coatings of group II; *e*, close-packed spherulites making up layers of the coatings of group III; *f*, spherulite microlayers consisting of radially oriented columnar calcite crystals.

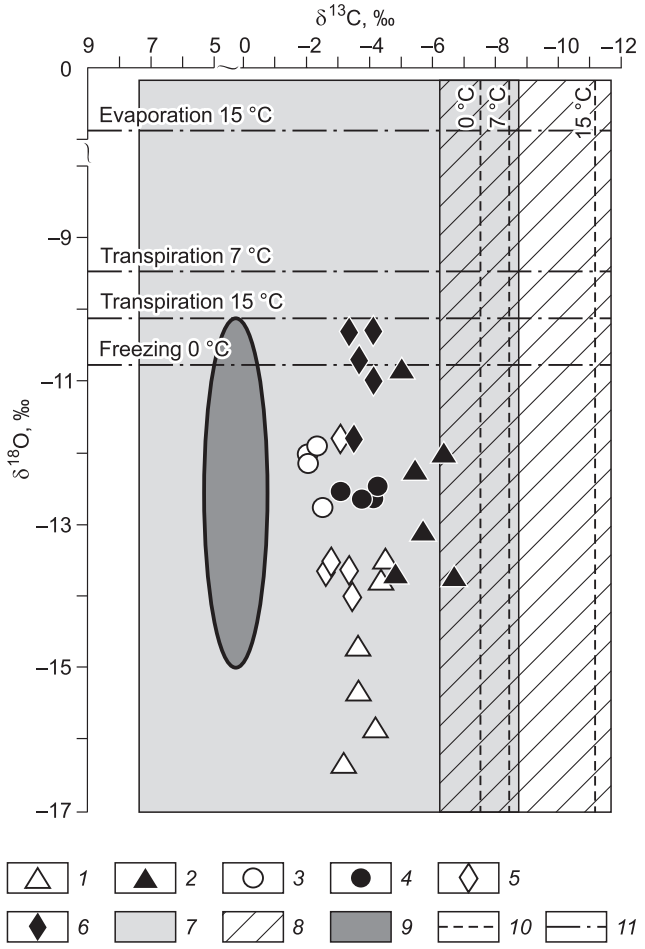

Fig. 7. Distribution of the theoretical and experimental values of $\delta^{13}C$ and $\delta^{18}O$ in carbonate coatings. *1*, inner layers of the coatings of group I; *2*, outer layers of the coatings of group I; *3*, inner layers of the coatings of group III; *4*, outer layers of the coatings of group III; *5*, inner layers of the coatings of group II; *6*, outer layers of the coatings of group II; *7*, theoretical interval of the $\delta^{13}C$ values for pedogenic carbonates; *8*, interval of the $\delta^{13}C$ values for carbonates forming in isotope equilibrium with soil CO_2; *9*, composition of stable carbon and oxygen isotopes for pedogenic carbonates forming in ice-marginal conditions (Cerling, 1984); *10*, limits of carbon isotope fractionation in pedogenic carbonates at different temperatures; *11*, limits of oxygen isotope fractionation in pedogenic carbonates at different temperatures.

accumulation rate being 0.6 mm/100 years. The coatings of group III are older, with the inner layers yielding the age of 34,860±790 cal. yr BP.

Composition of stable carbon isotopes in soil organic matter. The carbon isotope composition of soil organic matter directly depends on the type of vegetation, namely, on the specific features of its photosynthesis (Farquhar et al., 1989; Cerling and Quade, 1993). Most of the vegetation, including the majority of trees, herbs, and shrubs of the temperate zone, employs the Calvin cycle (C3 plants) in carbon fixation. The $\delta^{13}C$ values for their biomass range from –22 to –32‰ (Bowsher et al., 2008). In hot and arid conditions (deserts, semideserts, and dry steppes), more competitive plants use the Hatch–Slack pathway (C4 plants) and show $\delta^{13}C$ values of –10 to –18‰ (Bowsher et al., 2008).

The $\delta^{13}C$ values in the studied soils vary from –25.85 to –22.13‰ (Fig. 4). This suggests that soil organic matter has formed over the last 30–35 kyr from the biomass of C3 plants, which is typical of a temperate, extra-continental climate with subzero average annual temperatures. The carbon isotope composition of soil organic matter becomes heavier with increasing depth, reaching a maximum in the Karga pedosediments. The observed increase in the $\delta^{13}C$ values of the soils suggests an increase in the portion of C4 plants in ecosystems. However, their ecology (Bowsher et al., 2008) and the environmental conditions in the study area show that this is hardly possible.

The $\delta^{13}C$ and $\delta^{18}O$ values of pedogenic carbonate coatings. Pedogenic carbonates form in isotope equilibrium with soil CO_2, and their stable carbon isotope composition is in close correlation with the $\delta^{13}C$ value of soil organic matter. Note that carbon isotope fractionation in soils makes the carbon isotope composition of carbonates 14–16‰ heavier than that of soil organic matter. This is due to differences in diffusion coefficients between $^{13}CO_2$ and $^{12}CO_2$ (~4‰) and in the carbon fractionation factor between CO_2 and $CaCO_3$ (~10‰) (Cerling, 1984). Based on this pattern and the $\delta^{13}C$ values of organic matter from the studied soils, Fig. 7 shows a zone of isotope equilibrium, which must correspond to the $\delta^{13}C$ values of the coatings if they formed in equilibrium with soil CO_2. However, the $\delta^{13}C$ values of the outer layers of only two coatings of group I are in this zone, while the rest lie within the area of more positive values. This testifies to the lack of equilibrium with soil CO_2, the possible causes of which will be considered below.

In general, the $\delta^{13}C$ values for the coatings of group I vary from –6.80 to –3.25‰, decreasing in the outer layers, which are younger (Fig. 7; Table 2). The $\delta^{18}O$ values range from –16.33 to –10.95‰, increasing in the outer layers compared to the inner ones. The stable carbon isotope composition of the coatings of groups II and III is similar to but heavier than that of the coatings of group I. In the coatings of group III, $\delta^{13}C$ varies from –4.20 to –2.05‰, decreasing in the outer layers. The neoformations of group II show $\delta^{13}C$ values of –4.11 to –2.50‰, which also decrease in the outer layers compared to the inner ones. Substantial differences are observed in the oxygen isotope composition of the neoformations. In the coatings of group III, $\delta^{18}O$ varies from –12.63 to –11.99‰, slightly (by 0.5–0.6‰) decreasing in the outer layers; for the coatings of group II, this range is considerably wider (from –14.03 to –10.24‰). Note that $\delta^{18}O$ increases dramatically (by 3.0–3.5‰) in the outer layers.

DISCUSSION

Mechanisms of formation of carbonate coatings. The understanding of genesis of pedogenic carbonates is crucial for reconstruction of their formation conditions. One of the

Table 2. Stable carbon and oxygen isotope compositions of carbonate coatings

Coating no.	$\delta^{13}C$, ‰		$\delta^{18}O$, ‰	
	inner layer	outer layer	inner layer	outer layer
Group I				
Taiturka I				
1	–3.25	–4.73	–16.33	–13.58
2	–3.68	–5.04	–15.05	–11.2
3	–4.34	–5.41	–13.74	–10.95
Taiturka II				
4	–4.51	–5.78	–13.41	–13.01
5	–4.12	–6.8	–15.91	–13.83
6	–3.86	–6.3	–14.83	–11.99
Group II				
Taiturka I				
7	–3.3	–4.05	–13.68	–10.25
Taiturka II				
8	–2.6	–3.2	–13.74	–10.24
9	–2.83	–3.7	–13.61	–10.89
10	–3.4	–4.11	–14.03	–11.01
Lower Bulai II				
11	–2.5	–3.41	–13.89	–10.2
Group III				
Berezovyi				
12	–2.3	–4.2	–12.18	–12.57
13	–2.11	–3.96	–12.07	–12.61
Taiturka I				
14	–2.05	–3.14	–12.04	–12.52
15	–2.23	–4.1	–11.99	–12.63

best techniques for solving this problem is analysis of variations in the ratios of stable isotopes $^{12}C/^{13}C$ and $^{16}O/^{18}O$ in pedogenic carbonates, which reflect the different mechanisms and conditions of their formation (Cerling, 1984; Marion et al., 1991; Pustovoytov et al., 2007; Quade et al., 2007; Monger et al., 2009; Barta et al., 2018; and others). The carbon source in carbonates is CO_2, and the oxygen source is H_2O; consequently, the processes determining the water and carbon dioxide dynamics in soil control the isotopic composition of $CaCO_3$.

The main carbon sources in land ecosystems are the atmosphere and the breathing of plants and soil microorganisms. Note that the carbon isotope composition of atmospheric carbon dioxide is about –7‰. Plants dramatically fractionate carbon during photosynthesis; depending on the type of photosynthesis, soil is supplied with carbon with $\delta^{13}C$ values of –26±4‰ for C3 plants, –13±3‰ for C4 plants, and –32‰ to –15‰ for CAM plants (Bowsher et al., 2008). Soil freezing might affect carbon isotope composition both by release of CO_2 from the liquid phase and indirectly, because of the increased diffusion of atmospheric CO_2 into soil during periods of low biological activity (Quade et al., 1989; Marion et al., 1991).

So, the carbon isotope composition of soil CO_2 is determined by several factors: (1) the ratio between plants with different types of photosynthesis in the plant biomass; (2) soil respiration rate, which controls the intensity of diffusion of isotopically heavy atmospheric CO_2 into soil; (3) fractionation of $^{12}CO_2$ and $^{13}CO_2$ during migration in the soil profile because of different diffusion coefficients.

The oxygen isotope composition of soil water is determined by precipitation, the $\delta^{18}O$ value of which is closely related to the climatic conditions of the locality, particularly the average annual temperature. It is lighter at the cold high latitudes than at the warm low ones (Cerling and Quade, 1993). The oxygen isotope composition of soil water is almost constant during transpiration; however, evaporation causes considerable enrichment of residual water with heavy ^{18}O, whereas freezing results in its enrichment with light ^{16}O. The extent of isotopic fractionation in the above processes depends on temperature (Marion et al., 1991).

Thus, pedogenic carbonates can be enriched in one or another isotope compared to initial CO_2 or H_2O because of isotopic fractionation depending on the deposition mechanism and temperature conditions.

Three main mechanisms of soil carbonate deposition are proposed (Quade et al., 1989; Marion et al., 1991; Breecker et al., 2009; Peters et al., 2013):

(1) $CaCO_3$ is deposited on the soil surface during evaporation as a result of capillary rise of shallow groundwater. Carbon isotope composition is controlled in this case mainly by atmospheric CO_2; oxygen isotope composition, by meteoric precipitation and evaporation-related fractionation. Theoretically, the carbon and oxygen isotope compositions of depositing carbonates will become heavier during this process compared to those of soil organic matter and precipitation, respectively;

(2) $CaCO_3$ is deposited during transpiration-related soil drying. The carbon isotope composition of carbonates is controlled by soil CO_2; oxygen isotope composition, by atmospheric water. This will result in equilibrium $\delta^{13}C$ and $\delta^{18}O$ values with respect to soil CO_2 and oxygen of meteoric waters;

(3) $CaCO_3$ is deposited as soil solution freezes. Because of low biological activity, the carbon isotope composition of carbonates is controlled by the carbon isotope composition of atmospheric CO_2, and their oxygen isotope composition is controlled by precipitation and freezing-related oxygen fractionation. This will make the carbon isotope composition of carbonates heavier than that of soil organic matter and their oxygen isotope composition lighter than that of precipitation.

To reconstruct the mechanisms and conditions of deposition of carbonate coatings, we compared the experimental $\delta^{13}C$ and $\delta^{18}O$ values of secondary carbonate accumulations to theoretical values for different formation mechanisms (Fig. 7). The deposition of carbonates by different mechanisms can proceed at different temperatures, which has a dramatic influence on the value of isotopic fractionation in

the H_2O–CO_2–$CaCO_3$ system. We estimated factors of isotopic fractionation during calcite deposition through freezing (0 °C), transpiration (7 and 15 °C), and evaporation (15 °C) using equations from (Cerling, 1984; Marion et al., 1991).

The upper limit of carbon isotope fractionation was taken as –7‰ (the $\delta^{13}C$ value of atmospheric carbon). The average measured $\delta^{13}C$ values of vegetation for the study area were –24‰, which was taken as the lower limit. Thus, the theoretical $\delta^{13}C$ values for pedogenic carbonates of the study locality must range from –8.8 to 7.4‰ (Fig. 6). Based on these data, the theoretical $\delta^{13}C$ values were calculated for calcite deposited at different temperatures: –8.6, –9.8, and –11.2‰ for 0,7, and 15 °C, respectively (Fig. 7).

To calculate the oxygen isotopic composition of pedogenic carbonates, the $\delta^{18}O$ value of meteoric waters is necessary. In the study area, it equals –11.13‰ (with respect to SMOW) and –40.73‰ (with respect to PDB) (Statistical…, 1992). The theoretical $\delta^{18}O$ values of carbonates deposited by concentration of soil solutions during transpiration were –9.33 and –10.13‰ at 7 and 15 °C, respectively. For evaporation concentration of soil solutions, the $\delta^{18}O$ value has to be about –0.73‰. In the case of freezing, the theoretical $\delta^{18}O$ values will become considerably smaller, about –10.73‰ (Fig. 7).

The carbon isotope composition of all the studied neoformations is within the range typical of pedogenic carbonates (Fig. 7). In almost all the cases, the $\delta^{13}C$ values are larger than equilibrium ones for acceptable temperatures, suggesting that atmospheric CO_2 made a serious contribution to the development of the studied neoformations. This regularity was earlier observed for carbonates forming in cool ice-marginal conditions (e.g., Cerling, 1984; Quade et al., 1989; Marion et al., 1991; Courty et al., 1994; Vogt et al., 2018), and the range of $\delta^{13}C$ values for these carbonates is even more positive. Relying on the data obtained, we presume that carbonate deposition took place during the degassing of soil solutions caused by a drastic change of environmental conditions in the course of periodic freezing–thawing processes, dynamic increase and decrease in the biological activity of soils, and alternating moistening of soil with meltwater and rain water and its subsequent drying, which could occur in the region in spring and autumn. However, the dynamics of all the above conditions in the isotopic composition of carbonates was overcome by the main factor, which is periodic freezing. This is why $\delta^{13}C$ values tending to the freezing mechanism are observed. Besides that, the $\delta^{18}O$ values decrease considerably, which is typical of calcite deposition during the freezing of soil solutions. These values in the studied carbonates are comparable with those forming in cool ice-marginal conditions (Fig. 7).

In addition, the submicromorphology of the coatings testifies to freezing-related calcite deposition. The formation of the crystals making up both the outer and inner layers presupposes high growth rate as a result of quick removal of the solvent, which was probably due to the freezing of soil solutions. This is especially evident in the layers in which spherulitic growth can be explained by crystal cleavage during crystallization from freezing solutions, and the needle-like shape of the subindividuals might be due to pseudomorphs after ice crystals (Vogt, 1991; Vogt and Corte, 1996). The carbonate groundmass of the coatings is divided into microlayers consisting of radially oriented columnar calcite crystals (Fig. 6*f*). This structure is considered a result of a pause in their growth, which left numerous small grains on the outer surface. The later resumption of growth provoked competition among arbitrarily oriented crystal seeds, which caused the formation of a radial-columnar texture (Broughton, 1983). Frequent interruptions of growth resulted in the appearance of a large number of microlayers replacing one another along abrupt contacts. These sharp breaks in the crystal growth might be due to periodic freezing of solutions from which they were deposited.

Thus, carbonate deposition took place during the degassing of soil solutions in the course of periodic freezing–thawing processes, dynamic increase and decrease in the biological activity of soils, and alternating moistening of soil with meltwater and rain water and its subsequent freezing, which could occur in the region in spring and autumn. Meltwater or rain water dissolved primary carbonates contained in the deposits; later, they crystallized as calcite in the course of soil freezing. In these conditions, carbon isotope composition was mainly influenced by atmospheric CO_2, and the oxygen isotope composition of carbonates was controlled by isotopic fractionation during the freezing of soil solutions. We detected no $\delta^{13}C$ and $\delta^{18}O$ values typical of the evaporation–transpiration mechanism.

Dynamics of soil formation conditions and climate fluctuations in the Late Neopleistocene and Holocene. The occurrence, morphology, and direct ^{14}C-AMS dating of layers of carbonate coatings show that the main time intervals of their formation in the study area belong to the Middle Holocene (3.6–3.3 cal. ka BP). The coatings of group I formed at that time, whereas the neoformations of groups II and III developed in the second half of the MIS 3 stage (24.1–23.3 and ~34–35 cal. ka BP, respectively).

The structure of the neoformations of group I permits distinguishing two main stages in their development. The inner layers of the coatings formed during the first stage. The increased content of organic matter and iron in these layers testifies to active humus illuviation into the BCA horizon and the Al–Fe–humus process in cool and humid conditions. The age of the described coating layers (3.6 cal. ka BP) corresponds to the cool and humid phase of development of pedogenic coatings (3.7 cal. ka BP) in cryoarid soils of Tuva (Bronnikova et al., 2017). The formation of the outer layers of the neoformations (second stage), which ended at 3.3 cal. ka BP, took place in the course of secondary illuvial redistribution of carbonates in dry climatic conditions. The material of the coatings crystallized from solutions highly saturated with carbonates. This is evidenced by the small crystals making up the coatings which show no signs of etching and

dissolution. The high $CaCO_3$ content might be due to a temperature rise manifested in the decreased solubility of CO_2 and its increased content in soil air as a result of increased biological activity. The rates of formation of pedogenic carbonates increased substantially in such conditions (Zamanian et al., 2016). Also, aridization at this stage is confirmed by the character of change in the stable carbon and oxygen isotope compositions in the coating layers. The $\delta^{13}C$ values decrease in the outer layers compared to the inner ones, while the $\delta^{18}O$ values in younger layers of the coatings increase, suggesting gradual enrichment of local precipitation with ^{18}O (Golubtsov et al., 2014). Such changes were caused by aridization and an increase in the average annual temperatures, which is also evidenced at that time by pedolithological data (Vorob'eva, 2010), a decrease in the diatom content of deposits of Lake Kotokel', their heavier oxygen isotope composition (Kostrova et al., 2016), and the humidity dynamics in the Baikal region and adjacent areas (Wang and Feng, 2013) (Fig. 8).

The formation of the coatings of groups II and III chronologically corresponds to two regional soil formation levels (Lower Osa and Upper Osa) (Vorob'eva, 2010) and an increase in the diatom content of bottom deposits of Lake Kotokel' as their oxygen isotope composition becomes

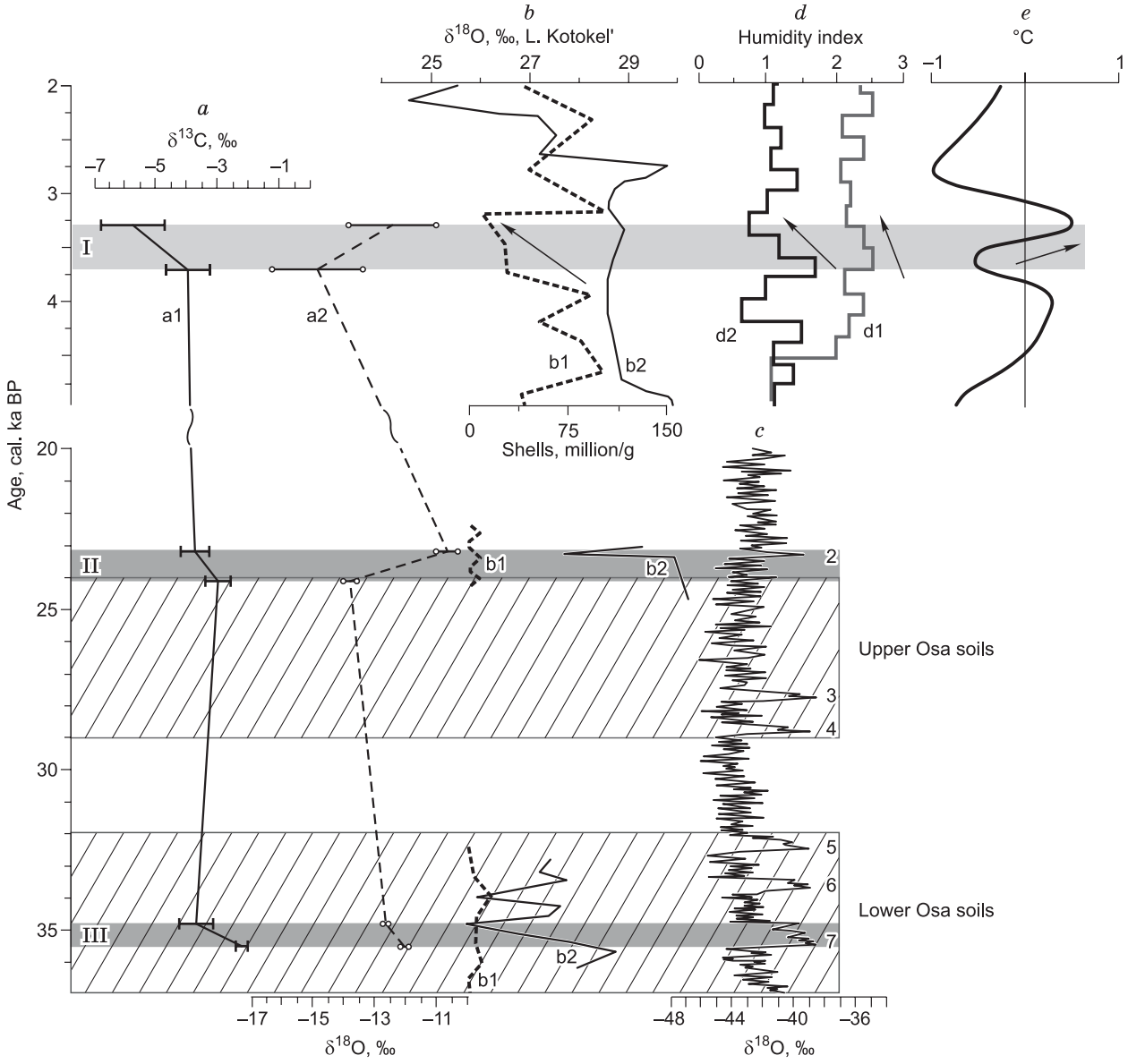

Fig. 8. Correlation of the formation stages of carbonate coatings with regional and global paleoclimate records. *a*, Composition of stable carbon (a1) and oxygen (a2) isotopes in pedogenic carbonate coatings; *b*, content of diatom shells (b1) and their oxygen isotope composition (b2) in the bottom sediments of Lake Kotokel' (Kostrova et al., 2016); *c*, NGRIP oxygen isotope scale as a proxy of atmospheric temperatures in the Northern Hemisphere (numbers show positive shifts in D–O events) (Svensson et al., 2008); *d*, humidity dynamics in northern Mongolia (d1) and the Baikal region (d2) (Wang and Feng, 2013); *e*, temperature dynamics in Cisbaikalia (Vorob'eva, 2010). Roman numbers in the left part of the figure indicate the groups of coatings and the intervals of their formation.

heavier, at 36–32 cal. ka BP and during MIS 2 (Kostrova et al., 2016). The listed stages correlate with short intervals in D–O events (2 and 7), which reflect an increase in the average air temperature in the Northern Hemisphere (Svensson et al., 2008) (Fig. 8). The MIS 3 coatings formed considerably more slowly than the Holocene neoformations (0.6 mm/100 years vs. 2 mm/100 years, respectively). The formation of pedogenic carbonates is much more intense in the case of a temperature increase, which implies the decreased solubility of CO_2 and its increased concentration in soil air as a result of higher biological activity (Zamanian et al., 2016); this suggests the lower heat supply of Karga (MIS 3) soils and, probably, the more humid climatic conditions of the Karga megainterstadial in the study area. This hypothesis is confirmed by the morphology and composition of the neoformations. The coatings of groups II and III are richer in admixtures of organic matter, which, most probably, penetrated the BCA horizons of soils more actively at that time. The coatings formed in the late Middle Holocene and Late Karga (MIS 3) epoch show similar ratios of stable carbon and oxygen isotope compositions. Considering the decisive influence of periodic freezing–thawing processes of soils on the isotopic composition of the coatings, we assume that the temperatures of pedogenesis in these epochs were the same, mainly because the soils received little heat and were seasonally frozen for a long time.

CONCLUSIONS

Three groups of carbonate coatings are distinguished based on the occurrence, morphology, and material and isotopic compositions. Direct ^{14}C AMS dating of the microlayers of the coatings permitted distinguishing the intervals of their formation. The coatings of group I formed in the Middle Holocene (3.6–3.3 cal. ka BP), and the coatings of groups II and III, in the second half of MIS 3 (24.1–23.3 and ~34–35 cal. ka BP, respectively).

The paleoecologic conditions reconstructed for the established stages of carbonate coating formation correlate with the course of climatic fluctuations in the region and in the Northern Hemisphere as a whole. They reflect the influence of temperature and humidity fluctuations on the dynamics of soil formation processes. In general, the intervals of coating formation correspond to short phases of temperature rise and reflect the climate dynamics within these phases. Based on analysis of the rates of coating formation and comparison of the isotopic composition of the coatings of different age groups, we assume that the climate in the Karga (MIS 3) megainterstadial was more humid than that in the Middle Holocene, with the temperatures of pedogenesis being the same. Both in the Middle Holocene and in the Karga epoch, the soils received little heat and were seasonally frozen for a long time.

Comparison of the age of the coatings with the age of recent and buried soils shows that the pedogenic carbonate coatings in the Upper Angara soils are a relict feature of the previous epochs of pedogenesis (MIS 3) and the first stages of recent soil formation, which began, most likely, in the Middle Holocene. As the age of the neoformations always corresponds to the age of host sediments, coatings can be regarded as a significant chronological proxy.

The data obtained are an important source of paleoclimatic information, supplementing and specifying paleogeographical data. The study of carbonate coatings permits obtaining information on paleoclimate fluctuations within narrow time intervals, which is especially important for prediction of climatic and environmental changes in the nearest future.

The study was conducted under a research program (0347-2016-0002) of V.B. Sochava Institute of Geography, Siberian Branch of the Russian Academy of Sciences, and supported by the Russian Foundation for Basic Research (project no. 17-04-00092).

REFERENCES

Aleksandrovskii, A.L., 2008. Environmental record in Holocene soils, in: Targul'yan, V.O., Goryachkin, S.V. (Eds.), Soil Memory: Soil as a Record of Biosphere–Geosphere–Anthroposphere Interactions [in Russian]. LKI, Moscow, pp. 75–105.

Alexandrovskiy, A.L., Chichagova, O.A., 1998. Radiocarbon age of Holocene paleosols of the East European forest–steppe zone. Catena 34 (1–2), 197–207.

Alekseeva, T.V., Alekseev, A.O., Gubin, S.V., Kabanov, P.B., Alekseeva, V.A., 2016. Palaeoenvironments of the Middle–Late Mississippian Moscow Basin (Russia) from multiproxy study of palaeosols and palaeokarsts. Palaeogeogr. Palaeoclimatol. Palaeoecol. 450, 1–16.

Amundson, R., Wang, Y., Chadwick, O., Trumbore, S., McFadden, L., McDonald, E., Wells, S., DeNiro, M., 1994. Factors and processes governing the ^{14}C content of carbonate in desert soils. Earth Planet. Sci. Lett. 125 (1–4), 385–405.

Antropov, P.Ya. (Ed.), 1962. Geology of the Soviet Union [in Russian], Vol. 17: The Irkutsk Region. Gosgeoltekhizdat, Moscow.

Barta, G., Bradák, B., Novothny, Á., Markó, A., Szeberényi, J., Kiss, K., Kovács, J., 2018. The influence of paleogeomorphology on the stable isotope signals of paleosols. Geoderma 330, 221–231.

Birkeland, P.W., 1999. Soils and Geomorphology. Oxford Univ. Press, New York.

Bowsher, C., Steer, M., Tobin, A., 2008. Plant Biochemistry. Garland Publ., New York.

Breecker, D.O., Sharp, Z.D., McFadden, L.D., 2009. Seasonal bias in the formation and stable isotopic composition of pedogenic carbonate in modern soils from central New Mexico, USA. Geol. Soc. Am. Bull. 121 (3–4), 630–640.

Brewer, R., 1964. Fabric and Mineral Analysis of Soils. John Wiley & Sons, New York, London, Sydney.

Brock, A.L., Buck, B.J., 2005. A new formation process for calcic pendants from Pahranagat Valley, Nevada, USA, and implication for dating Quaternary landforms. Quat. Res. 63 (3), 359–367.

Bronnikova, M.A., 2008. Silicate coatings of illuviation as archives of soil memory, in: Targul'yan, V.O., Goryachkin, S.V. (Eds.), Soil Memory: Soil as a Record of Biosphere–Geosphere–Anthroposphere Interactions [in Russian]. LKI, Moscow, pp. 468–497.

Bronnikova, M.A., Konoplianikova, Yu.V., Agatova, A.R., Zazovskaya, E.P., Lebedeva, M.P., Turova, I.V., Nepop, R.K., Shorkunov, I.G., Cherkinsky, A.E., 2017. Coatings in cryoaridic soils and other records of landscape and climate changes in the Ak-Khol Lake basin (Tyva). Eurasian Soil Sci. 50 (2), 142–157.

Broughton, P.L., 1983. Environmental implications of competitive growth fabrics in stalactitic carbonate. Int. J. Speleol. 13 (1–4), 31–41.

Cerling, T.E., 1984. The stable isotopic composition of soil carbonate and its relationship to climate. Earth Planet. Sci. Lett. 71, 229–240.

Cerling, T.E., Quade, J., 1993. Stable carbon and oxygen isotopes in soil carbonates, in: Swart, P.K., Lohmann, K.C., Mckenzie, J., Savin, S. (Eds.), Climate Change in Continental Isotopic Records. Geophys. Monograph Ser. AGU, Washington, D.C., Vol. 78, pp. 217–231.

Chadwick, O.A., Graham, R.C., 2000. Pedogenic processes, in: Sumner, M.E. (Ed.), Handbook of Soil Science. CRC Press, Boca Raton, Fla., pp. 41–75.

Chen, Y., Polach, H.A., 1986. Validity of ^{14}C ages of carbonate in sediments. Radiocarbon 28 (2A), 464–472.

Courty, M.-A., Marlin, C., Dever, L., Tremblay, P., Vachier, P., 1994. The properties, genesis and environmental significance of calcitic pendents from the High Arctic (Spitsbergen). Geoderma 61 (1–2), 71–102.

Deutz, P., Montañez, I.P., Monger, H.C., 2002. Morphology and stable and radiogenic isotope composition of pedogenic carbonates in late Quaternary relict soils, New Mexico, U.S.A.: an integrated record of pedogenic overprinting. J. Sediment. Res. 72 (6), 809–822.

Dworkin, S.I., Nordt, L., Atchley, S., 2005. Determining terrestrial paleotemperatures using the oxygen isotopic composition of pedogenic carbonate. Earth Planet. Sci. Lett. 237 (1–2), 56–68.

Ermolova, N.M., 1978. The Late Anthropogene Theriofauna of the Angara Valley [in Russian]. Nauka, Novosibirsk.

Eswaran, H., Reich, P.F., Kimble, J.M., Beinroth, F.H., Padmanabhan, E., Moncharoen, P., 2000. Global carbon sinks, in: Lal, R., Kimble, J.M., Eswaran, H., Stewart, B.A. (Eds.), Global Climate Change and Pedogenic Carbonates. CRC Press, Boca Raton, Fla., pp. 15–26.

Fairchild, I.J., Baker, A., 2012. Speleothem Science: From Process to Past Environments. Wiley–Blackwell, Chichester.

Farquhar, G.D., Ehleringer, J.R., Hubick, K.T., 1989. Carbon isotope discrimination and photosynthesis. Annu. Rev. Plant Physiol. Plant Mol. Biol. 40 (1), 503–537.

Feng, Z.-D., Ran, M., Yang, Q.L., Zhai, X.W., Wanga, W., Zhang, X.S., Huang, C.Q., 2011. Stratigraphies and chronologies of late Quaternary loess–paleosol sequences in the core area of the central Asian arid zone. Quat. Int. 240 (1–2), 156–166.

Florensov, N.A. (Ed.), 1971. Plateaus and Lowlands of East Siberia [in Russian]. Nauka, Moscow.

Glushankova, N.I., 2010. The paleopedological method, in: Kaplin, P.A., Yanina, T.A. (Eds.), Methods of Paleogeographical Reconstructions [in Russian]. Geograficheskiy Fakul'tet Mosk. Gos. Univ., Moscow, pp. 38–59.

Golubtsov, V.A., 2017. Secondary carbonate accumulations in soils of the Baikal region: formation processes and significance for paleosoil investigations. Tomsk State Univ. J. Biol., No. 39, 6–28.

Golubtsov, V.A., Cherkashina, A.A., Pustovoytov, K.E., Stahr, K., 2014. Stable carbon and oxygen isotopes in pedogenic carbonate coatings of chernozems in the Southern Cis-Baikalia as indicators of local environmental changes. Eurasian Soil Sci. 47 (10), 1015–1026.

Irkutsk Climate, http://www.pogodaiklimat.ru/climate/30710.htm.

Khokhlova, O.S., 2008. Pedogenic carbonates as proxies of soil formation conditions (example of the steppe zone of the East European Plain), in: Targul'yan, V.O., Goryachkin, S.V. (Eds.), Soil Memory: Soil as a Record of Biosphere–Geosphere–Anthroposphere Interactions [in Russian]. LKI, Moscow, pp. 406–437.

Khokhlova, O.S., Rusakov, A.V., Kuznetsova, A.M., Myakshina, T.N., Chendev, Yu.G., 2013. Radiocarbon dating of pedogenic carbonates in deep horizons of forest-steppe soils. Pochvovedenie, No. 9, 1095–1109.

Klement'ev, A.M., 2013. Late Karga faunae of the Irkut Amphitheater. Izv. Irkutsk. Univ., Ser. Geoarkheologiya. Etnologiya. Antropologiya, No. 1 (2), 30–43.

Kostrova, S.S., Meyer, H., Tarasov, P.E., Bezrukova, E.V., Chapligin, B., Kossler, A., Pavlova, L.A., Kuzmin, M.I., 2016. Oxygen isotope composition of diatoms from sediments of Lake Kotokel (Buryatia). Russian Geology and Geophysics (Geologiya i Geofizika) 57 (8), 1239–1247 (1571–1580).

Kovda, I.V., Wilding, L.P., Drees, L.R., 2003. Micromorphology, submicroscopy and microprobe study of carbonate pedofeatures in a Vertisol gilgai soil complex, South Russia. Catena 54 (3), 457–476.

Kovda, I., Mora, C.I., Wilding, L.P., 2006. Stable isotope compositions of pedogenic carbonates and soil organic matter in a temperate climate Vertisol with gilgai, southern Russia. Geoderma 136 (1–2), 423–435.

Kraus, M.J., 1999. Paleosols in clastic sedimentary rocks: their geologic applications. Earth Sci. Rev. 47 (1–2), 41–70.

Logachev, N.A., Lomonosova, T.K., Klimanova, V.M., 1964. Cenozoic Deposits of the Irkut Amphitheater [in Russian]. Nauka, Moscow.

Marion, G.M., Introne, D.S., Van Cleve, K., 1991. The stable isotope geochemistry of $CaCO_3$ on the Tanana River floodplain of interior Alaska, U.S.A.: Composition and mechanisms of formation. Chem. Geol. (Isot. Geosci. Sect.) 86 (2), 97–110.

Monger, H.C., Cole, D.R., Buck, B.J., Gallegos, R.A., 2009. Scale and the isotopic record of C4 plants in pedogenic carbonate: from the biome to the rhizosphere. Ecology 90 (6), 1498–1511.

Murphy, L.R., Hurst, S.C., Holliday, V.T., Johnson, E., 2014. Late Quaternary landscape evolution, soil stratigraphy, and geoarchaeology of the Caprock Canyonlands, Northwest Texas, USA. Quat. Int. 342, 57–72.

Oerter, E.J., Amundson, R., 2016. Climate controls on spatial and temporal variations in the formation of pedogenic carbonate in the western Great Basin of North America. Geol. Soc. Am. Bull. 128 (7), B31367.1.

Oerter, E.J., Sharp, W.D., Oster, J.L., Ebeling, A., Valley, J.W., Kozdon, R., Orland, I.J., Hellstrom, J., Woodhead, J.D., Hergt, J.M., Chadwick, O.A., Amundson, R., 2016. Pedothem carbonates reveal anomalous North American atmospheric circulation 70,000–55,000 years ago. Proc. Natl. Acad. Sci. U.S.A. 113 (4), 919–924.

Pendall, E.G., Harden, J.W., Trumbore, S.E., Chadwick, O.A., 1994. Isotopic approach to soil carbonate dynamics and implications for paleoclimatic interpretations. Quat. Res. 42 (1), 60–71.

Peters, N.A., Huntington, K.W., Hoke, G.D., 2013. Hot or not? Impact of seasonally variable soil carbonate formation on paleotemperature and O-isotope records from clumped isotope thermometry. Earth Planet. Sci. Lett. 361, 208–218.

Pustovoytov, K., 2002. Pedogenic carbonate cutans on clasts in soils as a record of history of grassland ecosystems. Palaeogeogr. Palaeoclimatol. Palaeoecol. 177 (1–2), 199–214.

Pustovoytov, K., Schmidt, K., Taubald, H., 2007. Evidence for Holocene environmental changes in the northern Fertile Crescent provided by pedogenic carbonate coatings. Quat. Res. 67 (3), 315–327.

Quade, J., Cerling, T., Bowman, J., 1989. Systematic variations in the carbon and oxygen isotopic composition of pedogenic carbonate along elevation transects in the southern Great Basin, United States. Geol. Soc. Am. Bull. 101 (4), 464–475.

Quade, J., Garzione, C., Eiler, J., 2007. Paleoelevation reconstruction using pedogenic carbonates. Rev. Mineral. Geochem. 66 (1), 53–88.

Quade, J., Eiler, J., Daëron, M., Achyuthan, H., 2013. The clumped isotope geothermometer in soil and paleosol carbonate. Geochim. Cosmochim. Acta 105, 92–107.

Reeder, R.J. (Ed.), 1983. Carbonates: Mineralogy and Chemistry. Reviews in Mineralogy. Mineralogical Society of America, Washington, D.C.

Retallack, G.J., 2001. Soils of the Past: An Introduction to Paleopedology, Blackwell, Oxford.

Sauer, D., Kadereit, A., Kühn, P., Koesel, M., Miller, C.E., Shinonaga, T., Kreutzer, S., Herrmann, L., Fleck, W., Starkovich, B.M., Stahr, K., 2016. The loess-palaeosol sequence of Datthausen, SW

Germany: Characteristics, chronology, and implications for the use of the Lohne Soil as a marker soil. Catena 146, 10–29.

Sharp, W.D., Ludwig, K.R., Chadwick, O.A., Amundson, R., Glaser, L.L., 2003. Dating fluvial terraces by ^{230}Th/U on pedogenic carbonate, Wind River Basin, Wyoming. Quat. Res. 59 (2), 139–150.

Sheldon, N.D., Tabor, N.J., 2009. Quantitative paleoenvironmental and paleoclimatic reconstruction using paleosols. Earth Sci. Rev. 95 (1–2), 1–52.

Singhvi, A., Banerjee, D., Ramesh, R., Rajaguru, S.N., Gogte, V., 1996. A luminescence method for dating 'dirty' pedogenic carbonates for paleoenvironmental reconstruction. Earth Planet. Sci. Lett. 139 (1–2), 321–332.

Statistical treatment of data on environmental isotopes in precipitation, 1992, in: Technical Report Series No. 331. International Atomic Energy Agency, Vienna, p. 240.

Svensson, A., Andersen, K.K., Bigler, M., Clausen, H.B., Dahl-Jensen, D., Davies, S.M., Johnsen, S.J., Muscheler, R., Parrenin, F., Rasmussen, S.O., Röthlisberger, R., Seierstad, I., Steffensen, J.P., Vinther, B.M., 2008. A 60 000 year Greenland stratigraphic ice core chronology. Clim. Past 4 (1), 47–57.

Tabor, N.J., Myers, T.S., 2015. Paleosols as Indicators of Paleoenvironment and Paleoclimate. Annu. Rev. Earth Planet. Sci. 43 (1), 11.1–11.29.

Targul'yan, V.O., 2008. Soil memory: formation, proxies, and spatial and temporal diversity, in: Targul'yan, V.O., Goryachkin, S.V. (Eds.), Soil Memory: Soil as a Record of Biosphere–Geosphere–Anthroposphere Interactions [in Russian]. LKI, Moscow, pp. 24–57.

The Irkutsk–Cheremkhovo industrial area. 1969. Vostochno-Sibirskaya Pravda, Irkutsk, p. 64.

Vogt, T., 1991. Cryogenic physicochemical precipitations: Iron, silica, calcium carbonate. Permafrost Periglacial Processes 1, 283–293.

Vogt, T., Corte, A.E., 1996. Secondary precipitates in Pleistocene and present cryogenic environments (Mendoza Precordillera, Argentina, Transbaikalia, Siberia, and Seymour Island, Antarctica). Sedimentology 43 (1), 53–64.

Vogt, T., Clauer, N., Techer, I., 2018. The glaciogenic origin of the Pleistocene calcareous dust in Argentina on the basis of field, mineralogical, textural, and geochemical analyses. Quat. Res., 1–16.

Vorob'eva, G.A., 2010. Soil as a Record of Natural Events in Cisbaikalia: Problems of Soil Evolution and Classification [in Russian]. Izd. Irkutsk. Gos. Univ., Irkutsk.

Vorob'eva, G.A., Medvedev, G.I., 1985. Low terraces of the valleys of rivers of Baikal–Yenisei Siberia and Lake Baikal, in: The Genesis of Landforms [in Russian]. Nauka, Novosibirsk, pp. 144–153.

Wang, W., Feng, Z., 2013. Holocene moisture evolution across the Mongolian Plateau and its surrounding areas: A synthesis of climatic records. Earth Sci. Rev. 122, 38–57.

Wang, Y., McDonald, E., Amundson, R., McFadden, L., Chadwick, O., 1996. An isotopic study of soils in chronological sequences of alluvial deposits, Providence Mountains, California. Geol. Soc. Am. Bull. 108 (4), 379–391.

Williams, G.E., Polach, H.A., 1971. Radiocarbon dating of arid-zone calcareous paleosols. Geol. Soc. Am. Bull. 82 (11), 3069–3086.

Zamanian, K., Pustovoytov, K., Kuzyakov, Y., 2016. Pedogenic carbonates: Forms and formation processes. Earth Sci. Rev. 157, 1–17.

Zykina, V.S., Zykin, V.S., 2012. The Loess–Soil Succession and Evolution of the Environment and Climate of West Siberia in the Pleistocene [in Russian]. Geo, Novosibirsk.

Editorial responsibility: N.L. Dobretsov